Front. Earth Sci. 2018, 12(3): 625–639
https://doi.org/10.1007/s11707-018-0688-x

RESEARCH ARTICLE

Numerical simulation of hydrodynamic and water quality effects of shoreline changes in Bohai Bay

Han JIA[1], Yongming SHEN (✉)[1,2], Meirong SU[2], Chunxue YU[2]

1 State Key Laboratory of Coastal and Offshore Engineering, Dalian University of Technology, Dalian 116024, China
2 School of Environment and Civil Engineering, Dongguan University of Technology, Dongguan 523808, China

Abstract This study uses the HD and Ecolab modules of MIKE to simulate the hydrodynamic and water quality and predict the influence of shoreline changes in Bohai Bay, China. The study shows that shoreline changes weaken the residual current and generate a counter-clockwise circulation south of Huanghua Port, thereby resulting in weak water exchange capacity and low pollutant-diffusing capacity. Shoreline changes reduce the area of Bohai Bay, resulting in a smaller tidal prism and further weakening the water exchange capacity. This situation is not conducive to the diffusion of pollutants, and therefore may lead to increased water pollution in the bay. Shoreline changes hinder the spread of runoff, weaken the dilution effect of the river on seawater, and block the spread of coastal residual current, thereby resulting in increased salinity near the reclamation area. Shoreline changes lead to an increase in PO_4-P concentration and decrease in DIN concentration. The value of N/P near the project decreases, thereby weakening the phosphorus-limited effect.

Keywords Bohai Bay, shoreline changes, hydrodynamic, water quality

1 Introduction

Bohai Bay is located in the western part of the Bohai Sea, near the city of Tianjin and the provinces of Hebei and Shandong in China. Thus, it is an important political, economic, and cultural centre in the northern coastal area of the country. In recent years, with rapid economic development, the rise of reclamation activities has resulted in significant changes in the Bohai Bay shoreline (Wang et al., 2011b; Liu et al., 2014a; Wang et al., 2014). Although reclamation promotes economic development and eases the population pressure, there have been many ecological problems (Cai et al., 2014; Tian et al., 2016). As a typical semi-enclosed inner bay, Bohai Bay has a weak water exchange capacity, which causes difficulty for terrestrial pollutants to diffuse outward, thereby leading to serious pollution of coastal waters, affecting the regional ecology. This area is typical of the muddy gentle slope coast, and the pollutant transport along the coast driven by the tidal current is obvious. Water pollution changes the living environment of marine organisms (Wang et al., 2011a), decreases biological diversity, changes the structure of the community (Li et al., 2010), and has an impact on seabird migration (Yang et al., 2011), aquatic plants (Wang et al., 2012), and fisheries (Yan et al., 2013).

Thus, the influence of shoreline changes on hydrodynamic and water quality is an important research area that has received significant attention. In hydrodynamic research, numerous results have been obtained through data measurement and numerical simulation. For example, Kuang et al. (2012a, b) built a 2D morphological model to investigate the effect of reclamation on erosion and sedimentation in Caofeidian, north of Bohai Bay. Zhao and Sun (2013) used the SWAN model to study the change caused by reclamation of the wave fields in Bohai Bay, indicating that significant variations in wave fields occur in the harbour basin and tide channel.

In water quality research, however, studies mainly focus on the analysis of measured data. For example, Wang et al. (2009) collected water samples in 120 stations in the Bohai Sea and found that the high concentrations of dissolved inorganic nitrogen (DIN) and phosphate (PO_4-P) occurred in coastal waters, especially in the bays and some river estuaries. Similarly, Liu et al. (2014b) studied nutrient pollution status, change characteristics, and eutrophication by analysing water quality monitoring data of the red tide monitoring area in Tianjin. Huai et al. (2003) used the hybrid finite analytic (HFA) method to calculate the flow

Received June 19, 2017; accepted November 13, 2017

E-mail: ymshen@dlut.edu.cn

and water quality in estuaries and coastal waters, and checked the effectiveness of Komatsu's method for water purification (Huai et al., 2005). However, due to the complexity of water quality numerical simulation, the research has not advanced far enough, so building good models to simulate hydrodynamic and water quality have not yet been done.

This study simulates the hydrodynamics and water quality of Bohai Bay and uses a well-validated model to systematically analyze the influence of shoreline topography change and coastline variations of the reclamation project on the hydrodynamics and water quality in Bohai Bay. The results of this study can contribute to a decision basis for engineering design, environmental protection, and pollutant emission control.

2 Shoreline changes in Bohai Bay

The coast of Bohai Bay has undergone drastic changes in the past 10 years, the trend of which is from land to sea, and the land area has increased about 322 km^2; the coastline has grown about 331.6 km. The three regions with the most obvious changes are Tianjin Port, Caofeidian Port, and Huanghua Port, as shown in Fig. 1.

The increase in the coastline and land area of Tianjin Port area is very large, showing seaward progression. The land area increased about 105.5 km^2, the coastline grew about 101.1 km in the past 10 years. Caofeidian Port started reclamation in 2003, the land area increased about 172.8 km^2, the coastline grew about 102.2 km in the past 10 years. This area has the highest rate of seaward progression in Bohai Bay. The change in Huanghua Port is relatively small, the land area increased about 20.9 km^2, the coastline grew about 41.0 km in the past 10 years.

3 Model setup and verification

3.1 Model description

This study is based on the HD and Ecolab modules to simulate hydrodynamic and water quality and to predict the influences of shoreline changes in Bohai Bay. Bohai Bay is less than 30 meters deep. Even at the coastal engineering area, the average water depth is less than 5 meters. In these shallow water depth conditions, a 2-D model is selected in order to be more efficient. The model is based on the shallow water equations deduced from incompressible Reynolds averaged Navier-Stokes equations, subject to the assumptions of Boussinesq and of hydrostatic pressure.

The continuity equation is written as

$$\frac{\partial h}{\partial t}+\frac{\partial h\bar{u}}{\partial x}+\frac{\partial h\bar{v}}{\partial y}=hS, \tag{1}$$

and the two horizontal momentum equations for the x- and y-component, respectively:

$$\frac{\partial h\bar{u}}{\partial t}+\frac{\partial h\bar{u}^2}{\partial x}+\frac{\partial h\bar{v}\bar{u}}{\partial y}$$

$$=f\bar{v}h-gh\frac{\partial \eta}{\partial x}-\frac{h}{\rho_0}\frac{\partial p_a}{\partial x}-\frac{gh^2}{2\rho_0}\frac{\partial p}{\partial x}+\frac{\tau_{sx}}{\rho_0}-\frac{\tau_{bx}}{\rho_0}$$

$$-\frac{1}{\rho_0}\left(\frac{\partial s_{xx}}{\partial x}+\frac{\partial s_{xy}}{\partial y}\right)+\frac{\partial}{\partial x}(hT_{xx})+\frac{\partial}{\partial y}(hT_{xy})+hu_sS, \tag{2}$$

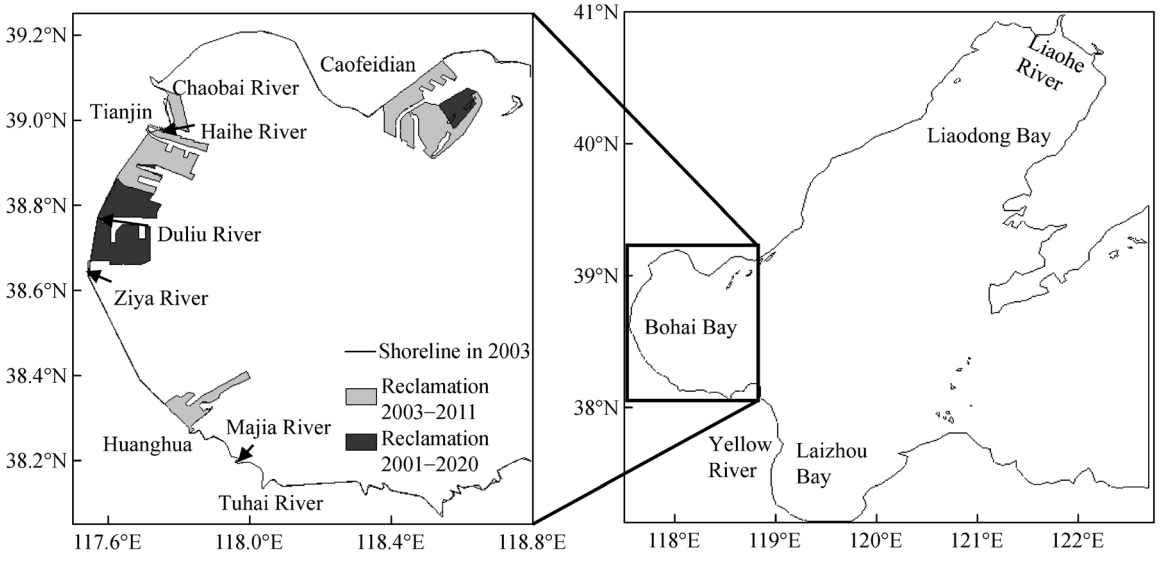

Fig. 1 Location and shoreline changes of Bohai Bay.

$$\frac{\partial h\overline{v}}{\partial t}+\frac{\partial h\overline{vu}}{\partial x}+\frac{\partial h\overline{v}^2}{\partial y}$$

$$=-f\overline{u}h-gh\frac{\partial \eta}{\partial y}-\frac{h}{\rho_0}\frac{\partial p_a}{\partial y}-\frac{gh^2}{2\rho_0}\frac{\partial p}{\partial y}+\frac{\tau_{sy}}{\rho_0}-\frac{\tau_{by}}{\rho_0}$$

$$-\frac{1}{\rho_0}\left(\frac{\partial s_{yx}}{\partial x}+\frac{\partial s_{yy}}{\partial y}\right)+\frac{\partial}{\partial x}(hT_{xy})+\frac{\partial}{\partial y}(hT_{yy})+hv_sS, \quad (3)$$

where x and y are the Cartesian co-ordinates; t is the time; $h=\eta+d$ is the total water depth; η is the surface elevation; d is the still level; $\overline{u}$ and $\overline{v}$ are the depth-averaged velocity components in the x and y directions; S is the magnitude of the discharge due to point sources; f is the Coriolis parameter; ρ_0 is the water density; p_a is the atmospheric pressure; g is the gravitational acceleration; (u_s,v_s) are the velocity components in the x and y directions, by which the water is discharged into the ambient water; T_{xx}, T_{xy} (T_{yx}), and T_{yy} are the components of the radiation stress tensor; (τ_{sx},τ_{sy}) and (τ_{bx},τ_{by}) are the x and y components of the surface wind and bottom stresses.

The transport equations for salt and temperature are:

$$\frac{\partial h\overline{T}}{\partial t}+\frac{\partial h\overline{u}\overline{T}}{\partial x}+\frac{\partial h\overline{v}\overline{T}}{\partial y}=hF_T+h\hat{H}+hT_sS, \quad (4)$$

$$\frac{\partial h\overline{s}}{\partial t}+\frac{\partial h\overline{u}\overline{s}}{\partial x}+\frac{\partial h\overline{v}\overline{s}}{\partial y}=hF_s+hs_sS, \quad (5)$$

where $\overline{T}$ and $\overline{s}$ are the depth-averaged temperature and salinity; $\hat{H}$ is a source term due to heat exchange with the atmosphere; T_s and s_s are the temperature and the salinity of the source; F_T and F_s are the horizontal diffusion terms of temperature and the salinity.

The transport equation for water quality state variable is:

$$\frac{\partial h\overline{c}}{\partial t}+\frac{\partial h\overline{uc}}{\partial x}+\frac{\partial h\overline{vc}}{\partial y}=hF_c+hc_sS+hP_c, \quad (6)$$

where $\overline{c}$ is the concentration of the ECO Lab (water quality) state variable. In this study, the state variables are biochemical oxygen demand (BOD), dissolved oxygen (DO), ammonium (NH_4-N), nitrite (NO_2-N), nitrate (NO_3-N), phosphorus (PO_4-P) and Chlorophyll-a (Chl-a); F_c is the horizontal diffusion term of this state variable; c_s is the state variable of the source; P_c is the ECO Lab processes, the equation is

$$P_c=\frac{\mathrm{d}c}{\mathrm{d}t}=\sum_{t=1}^{n}\mathrm{process}_t, \quad (7)$$

where $\mathrm{process}_t$ is a biochemical process of this state variable; n is the number of biochemical processes of this state variable. For example, there are 4 processes in Ammonium:

$$\frac{\mathrm{dNH_3}}{\mathrm{d}t}=+\text{ammonium yield from BOD decay}$$
$$-\text{transformation of ammonium to nitrate}$$
$$-\text{ammonium uptake by plants}$$
$$+\text{heterotroph respiration.} \quad (8)$$

It is well known that light penetrating into the water column affects the growth of phytoplankton. Therefore, the influence of water depth is set to control the ability of light to penetrate water.

3.2 Grids setup

A two-level unstructured triangular grid model is built as shown in Figs. 2 and 3. The topography data are based on

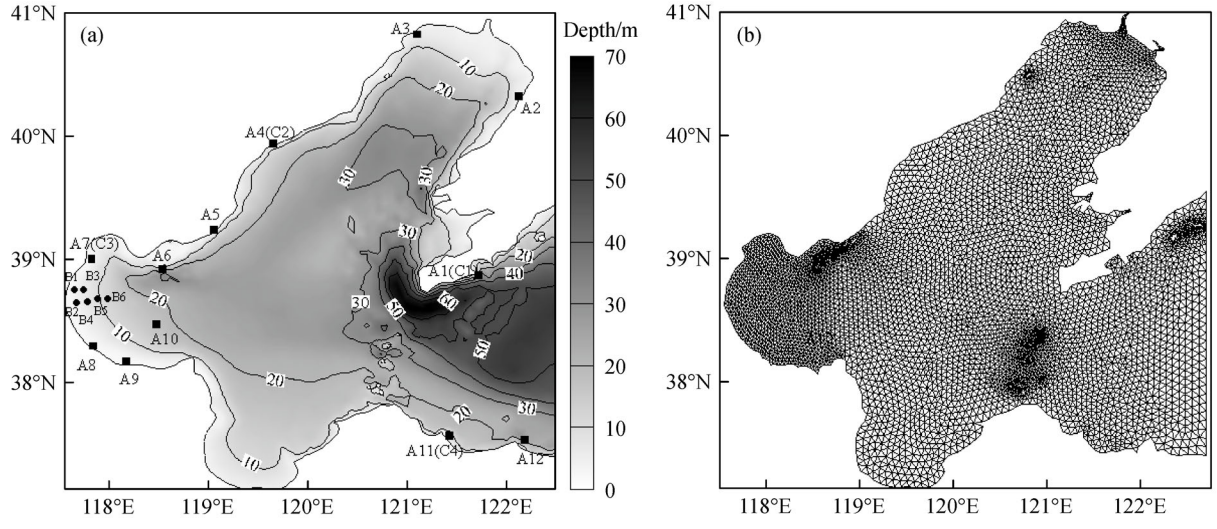

Fig. 2 The topography and locations of the observation stations (a) and the grid (b) of Bohai Sea (A1−A12: the tide level measured stations; B1−B6: the tide current measured stations; C1−C4: the temperature and salinity measured stations).

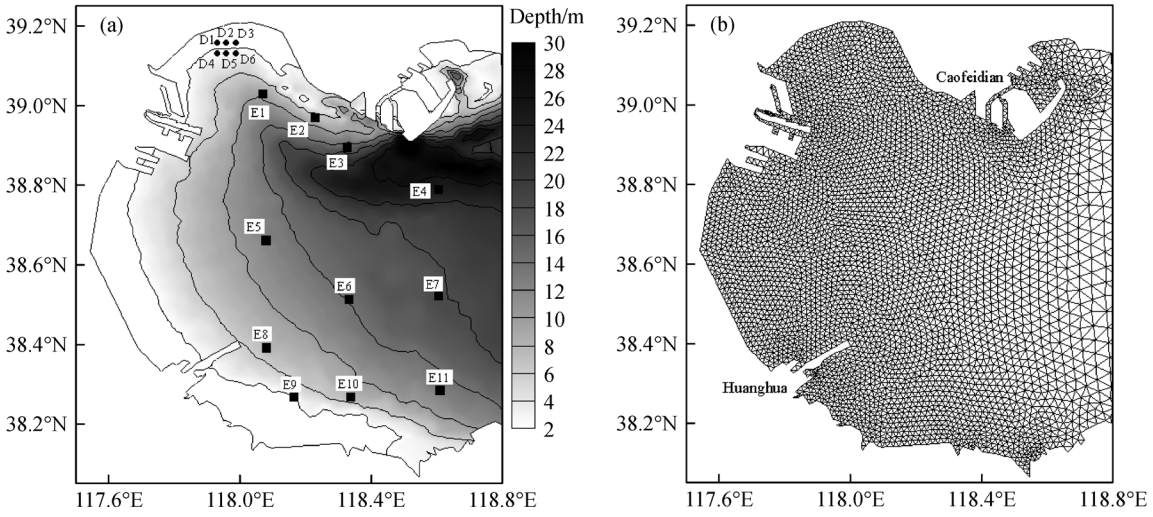

Fig. 3 The topography and locations of the observation stations (a) and the grid (b) of Bohai Bay (D1−D6: the water quality measured stations in red tide monitoring area of Tianjin; E1−E11: the water quality measured stations in cruise, May 2011).

the NOAA-ETOPO1 database, and the data resolution is 1/6° × 1/6°. The minimum grid length is 500 m (for the large grid) and 100 m (for the small grid). The large grid has 10,237 elements and covers the entire Bohai Sea within 37°–41.2°N, 117.5°–122.8°E. The small grid has 6824 elements and covers the Bohai Bay within 38°–39.2°N, 117.5°–118.8°E. The small grid can provide a high-resolution hydrodynamic field for the study area. Since Bohai Bay is part of the Bohai Sea, the nested technology is used in this model. To make this model more accurate, the large Bohai model is calculated, and then the data are extracted as the boundary and forced conditions of the Bohai Bay model.

3.3 Boundary conditions

For the tide boundary, tidal prediction software China Tide is used to calculate the nine tidal constituents (Sa, O_1, Q_1, K_1, P_1, N_2, M_2, S_2, and K_2) under given latitude and longitude coordinates by interpolation calculation and numerical calculation. According to Eq. (9), the software automatically calculates the required time-period tide series.

$$\eta = \sum_{i=1}^{n} f_i h_i \cos(\sigma_i t + \upsilon_{0i} + u_i - g_i),\ n = 9, \qquad (9)$$

where η is the tide level; h_i and g_i are the tidal harmonic constants (amplitude and retardation); σ_i is the angular velocity of the tide; t is the time; f_i is the tidal intersection factor; υ_{0i} is the first phase of astronomical tide; u_i is the tide intersection point of correction.

For the river boundary, although many rivers flow into the Bohai Sea, the runoff is generally small. According to runoff, the Bohai Sea model mainly considers the freshwater input of the Yellow, Liaohe, and Haihe rivers, and the runoff data are obtained from the *Chinese River Sediment Bulletin*. The Bohai Bay model considers the freshwater input of rivers such as Haihe, Chaobai, Duliu, Ziya, Majia, and Tuhai rivers (shown in Fig. 1).

For the temperature and salinity boundary, the temperature and salinity data of the open boundary of the Bohai Sea model are set to change with time and space. It comes from the global 1/12° reanalysis data on the HYCOM database. The temperature and salinity data on the HYCOM database at the boundary point were used to extract the boundary temperature and salinity data of the Bohai Sea model.

For the water quality boundary, the Bohai Bay model comprehensively considers seven types of state variables, such as BOD, DO, Chl-a, NH_4-N, NO_2-N, NO_3-N, and PO_4-P, and the data come from the Bohai Sea, Yellow Sea, East China Sea Atlas of the Oceans (Chemistry). Pollution sources consider the input of rivers such as the Haihe, Chaobai, Duliu, Ziya, Majia, and Tuhai.

For the sea surface boundary, the data are based on ECMWF database, and the data accuracy is 0.25° × 0.25°, including wind, temperature, relative humidity, clearness coefficient, evaporation, and precipitation.

3.4 Model parameters

To ensure that the model is stable, the simulation time of the model is from 00:00 on January 1, 2010 to 00:00 on January 1, 2012, during which the measurement data are available to verify the model. The second-year simulation data are selected after the model is stabilized for subsequent analysis. The time steps are in the 0.01 s to 60 s range. The critical CFL number is 0.8. The drying depth is 0.005 m, the flooding depth is 0.05 m, and the wetting depth is 0.1 m. The initial tidal level and flow

velocity are defined as 0 m and 0 m/s, respectively. The initial temperature and salinity are defined as annual average of 10.7°C and 30 PSU.

3.5 Model verification

In order to test the reliability of the model, the simulation results were verified by tide, tidal current, tidal harmonic constants, temperature, salinity, and water quality. Fig. 2(a) and Fig. 3(a) show the location of each verification station. Among them, A1–A12 are the tide level measuring stations, B1−B6 are the tide current measuring stations, C1–C4 are the temperature and salinity measuring stations, D1–D6 are the water quality measuring stations in red tide monitoring area of Tianjin, and E1–E11 are the water quality measuring stations in cruise during May 2011.

In model validation, the hydrodynamic and water quality are analyzed respectively. Tidal level, tidal current, O_1, K_1, M_2, S_2 constituents, temperature, and salinity are selected for hydrodynamic verification, DIN, PO_4-P, and N/P are selected for water quality verification.

The simulation tidal level data are compared with the measured data in mid-August 2011. The simulation tidal current data are compared with the measured data in mid-July 2011. The fitting results are good. Partial results of tidal level and tidal current verification are shown in Fig. 4 and Fig. 5.

In addition, the August tide simulation data of the entire Bohai Sea model elements are extracted to conduct harmonic analysis via MATLAB. Co-tidal charts of O_1, K_1, M_2, and S_2 constituents are drawn and are well matched with Bao et al. (2001) (Shown in Fig. 6).

Regression analysis of the tidal level and tidal current simulation data is conducted, and the RMSE (root mean square error) and R^2 of each station data are calculated, as shown in Tables 1 and 2. The error of each station is within 10% and R^2 is mostly larger than 0.8. The simulation results match the measured data well.

The simulated data for 2011 are selected for temperature and salinity verification when the model has been stabilized. The validation of temperature and salinity at the measuring stations are shown in Fig. 7. The regression analysis of temperature and salinity between simulation result and measured data is shown in Table 3. The simulation results match the measured data well. The distribution of temperature and salinity in summer and winter in the Bohai Sea are shown in Fig. 8. The distribution of temperature during the summer season is characterized by high temperature in the three bays and low temperature in the central. On the contrary, the

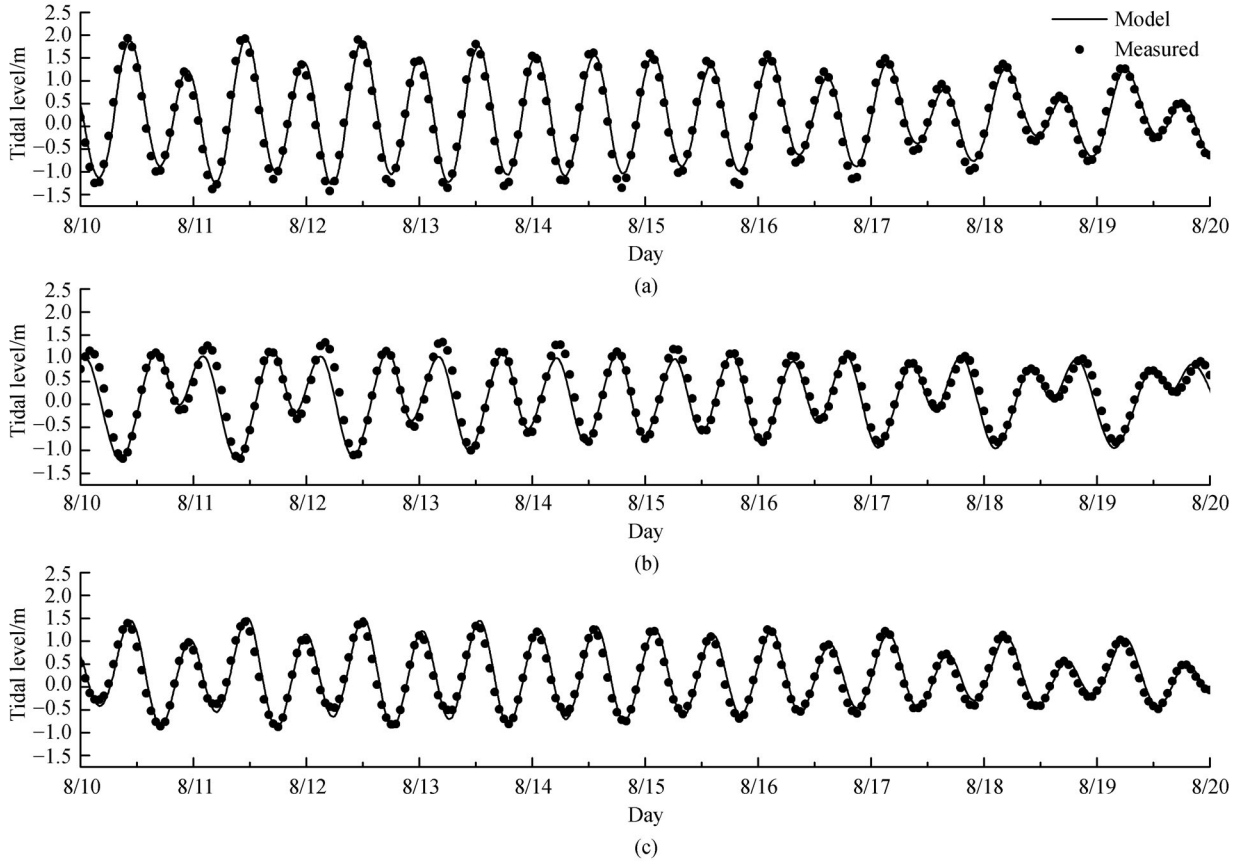

Fig. 4 The validation of tidal level at partial measured stations. (a) A1; (b) A6; (c) A12.

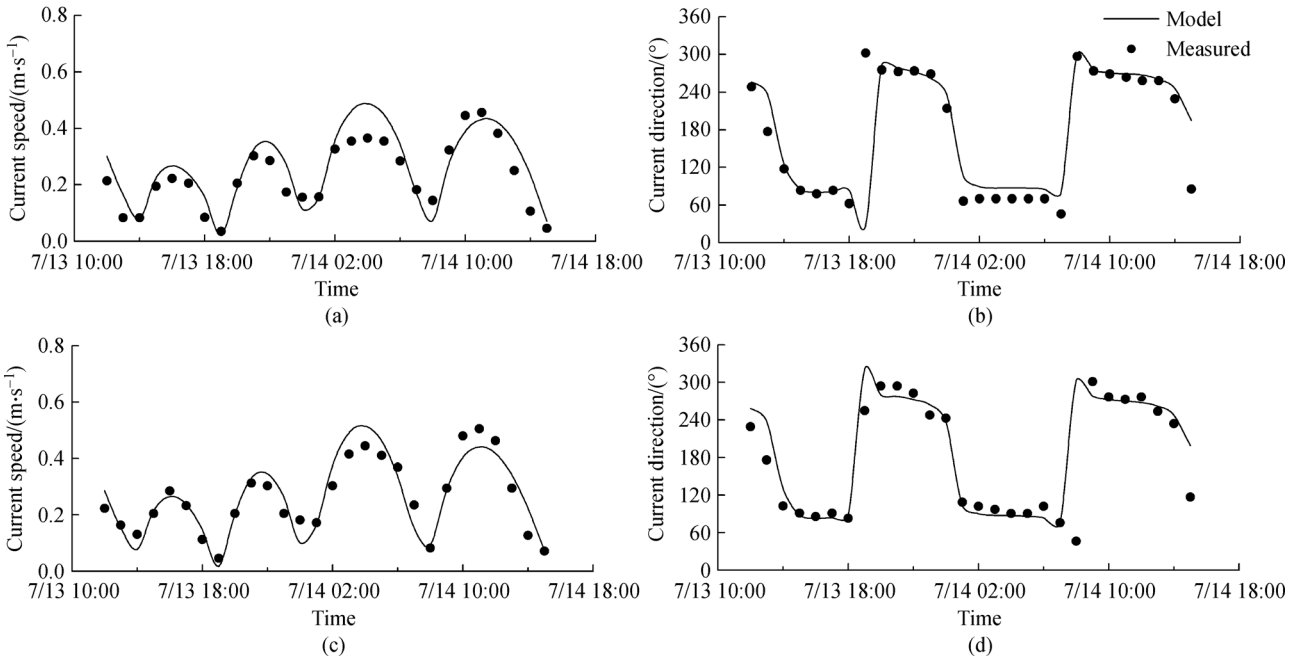

Fig. 5 The validation of tidal current at partial measured stations. (a) Current speed at B5; (b) current direction at B5; (c) current speed at B6; (d) current direction at B6.

distribution of temperature during the winter season is characterized by high temperature in the central and low temperature in the three bays. The distribution of salinity during the summer and winter seasons is characterized by high salinity in the central and northeast and relatively low salinity in the three bays. However, the salinity in the three bays is lower than that in winter due to the increased summer runoff, thereby resulting in the dilution of salt water. This condition is particularly evident in the estuary of the Yellow and Liaohe rivers.

Water quality simulation is based on the validated hydrodynamic model. The decoupling module is used to decouple the calculation, which avoids the problem of repeated calculation of the hydrodynamic part. This approach can significantly reduce the time of water quality simulation.

The water quality monitoring data on the Tianjin red tide monitoring area as reported by Liu et al. (2014b) and the measured data of the Bohai Bay area as reported by Li et al. (2012) are used for water quality verification. The simulated results of DIN and PO_4-P in the Tianjin red tide monitoring area are shown in Fig. 9. As the measured data are limited, the monthly data are used for verification. The monthly simulated results of six stations in the red tide monitoring area are extracted and the data are averaged to obtain the annual average variation curves of DIN and PO_4-P in this area. The value of the error bar represents the standard deviation of the simulation value, indicating the DIN and PO_4-P concentration range in this region. As shown in Fig. 9, most of the data are within the range of the error bars and the trend is consistent. Except for high measurements in a few months, the measured data and simulated results are well matched.

The distribution of DIN, PO_4-P, and Chlorophyll-a (Chl-a) in the spring of Bohai Bay are shown in Fig. 10. The DIN concentration distribution is characterised by a decrease from the high-value area of estuaries near the coast to the low-value area in the central and northeastern parts of the bay. The concentration gradient at the estuary is larger. The PO_4-P concentration distribution is characterised by the high-value area, which also appears near the estuary, and the concentration gradient is larger but the range is smaller than that of DIN. The concentration in the coastal area in the southwest is relatively small because of the smaller influence of runoff. The concentration from the centre to the eastern boundary of the sea area shows an increasing trend, which indicates that the high concentration area outside the Bohai Bay may be affected by the Yellow River runoff. The distribution of Chl-a concentration is characterised by the high-value area near the northwest estuary and gradually decreases to the southeast. The southern coast area affected by runoff also has a high-value area but it is lower than that in the northwest estuary. The concentration in the eastern and northeastern regions near the boundary is low. Comparison of the simulated distribution and measured data of Bohai Bay shows that the model is basically consistent with the measured results (Li et al., 2012).

The nitrogen to phosphorus ratio is an important indicator of water eutrophication. Redfield (1958) thinks that phytoplankton absorb inorganic nitrogen and phosphate nutrients at a 16:1 constant mole ratio. The water

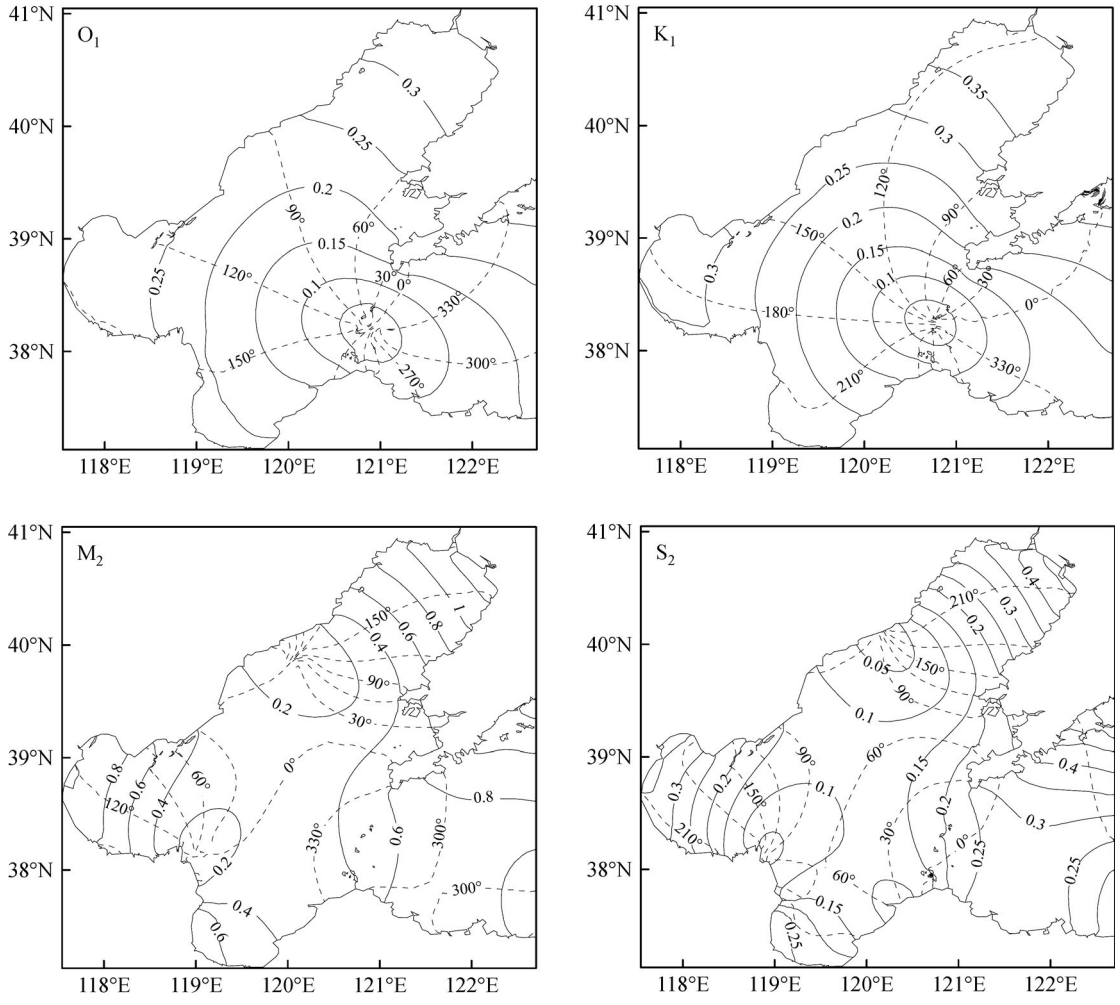

Fig. 6 Co-tidal charts of O_1, K_1, M_2, and S_2 constituents in the Bohai Sea (The solid line represents the amplitude, and the dashed line represents the angle).

Table 1 Regression analysis of the tidal level between simulation result and measured data

Measured station	Tidal level		Measured station	Tidal level	
	RMSE/m	R^2		RMSE/m	R^2
A1	0.2022	0.9190	A7	0.4175	0.7427
A2	0.3188	0.8819	A8	0.4005	0.6912
A3	0.2800	0.8709	A9	0.1918	0.9014
A4	0.1306	0.7999	A10	0.1586	0.9094
A5	0.1108	0.9232	A11	0.1680	0.9156
A6	0.1703	0.9151	A12	0.1627	0.9075

area is in phosphorus limit when the ratio is larger than 16, and the water area is in nitrogen limit when the ratio is less than 16. Liu et al. (2014b) have analysed water eutrophication in the Bohai Bay, and found that the eutrophication of Bohai Bay is serious, the content of inorganic nitrogen is at a high level, the content of phosphate is decreasing and the N/P ratio is much higher than 16, thereby showing a phosphorus-limited nutrient structure. Table 4 shows the N/P ratio measured at the E1–E11 monitoring stations and the simulated comparison results. The table shows that most parts of the Bohai Bay are in the phosphorus-limited nutrient structure, which is consistent with the measured results.

In summary, the nutrient and chlorophyll results in

Table 2 Regression analysis of the tidal current between simulation result and measured data

Measured station	Current speed		Current direction	
	RMSE/(m·s^{-1})	R^2	RMSE/(°)	R^2
B1	0.0843	0.7508	29.2180	0.8988
B2	0.0740	0.8199	27.4938	0.9114
B3	0.0653	0.7817	12.4841	0.9805
B4	0.0686	0.6942	23.0792	0.9374
B5	0.0583	0.8099	24.2951	0.9331
B6	0.0521	0.8605	26.6415	0.9174

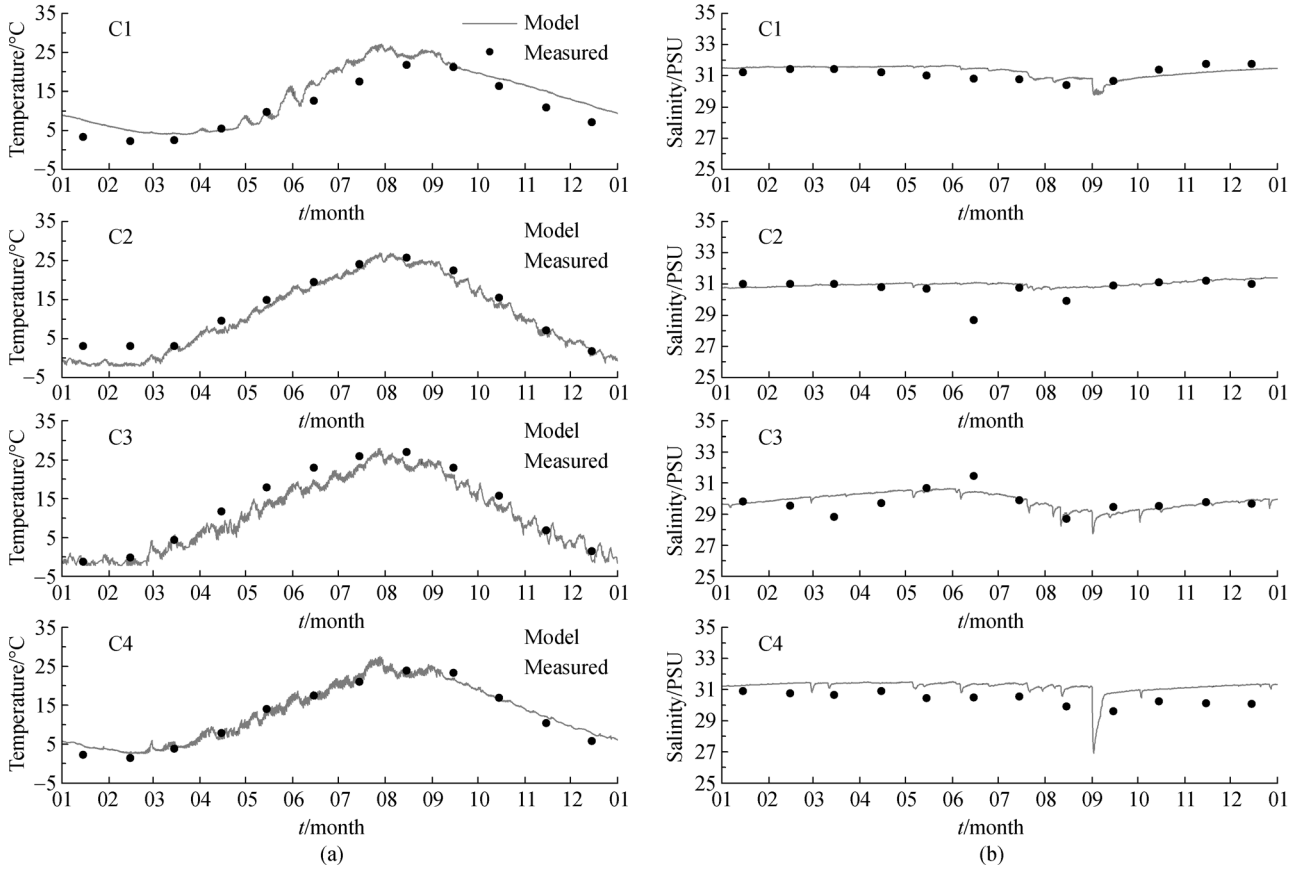

Fig. 7 The validation of (a) temperature and (b) salinity at measuring stations.

Bohai Bay simulated in this study are basically consistent with the measured results and findings of other scholars. The water quality model is reliable.

4 Results and discussion

To study the influence of shoreline changes on hydrodynamics and water quality, this paper takes the coastline topography of Bohai Bay in 2011 as the center to consider the reclamation projects of Tianjin, Caofeidian, and Huanghua ports. The grids are built for the natural coastline in 2003 and the expected shoreline in 2020 (shown in Fig. 11). Only the grids of the model were changed. The boundaries and other parameters were unchanged to control the variables and simulate them under the well-validated model.

4.1 Influence of runoff diffusion

Shoreline changes, especially reclamation work, have a significant impact on the spread of runoff after it reaches the estuary. This condition changes the flow direction and velocity of the river, thereby affecting the hydrodynamic and water quality of the surrounding waters. This phenomenon can be observed in the Haihe River. With

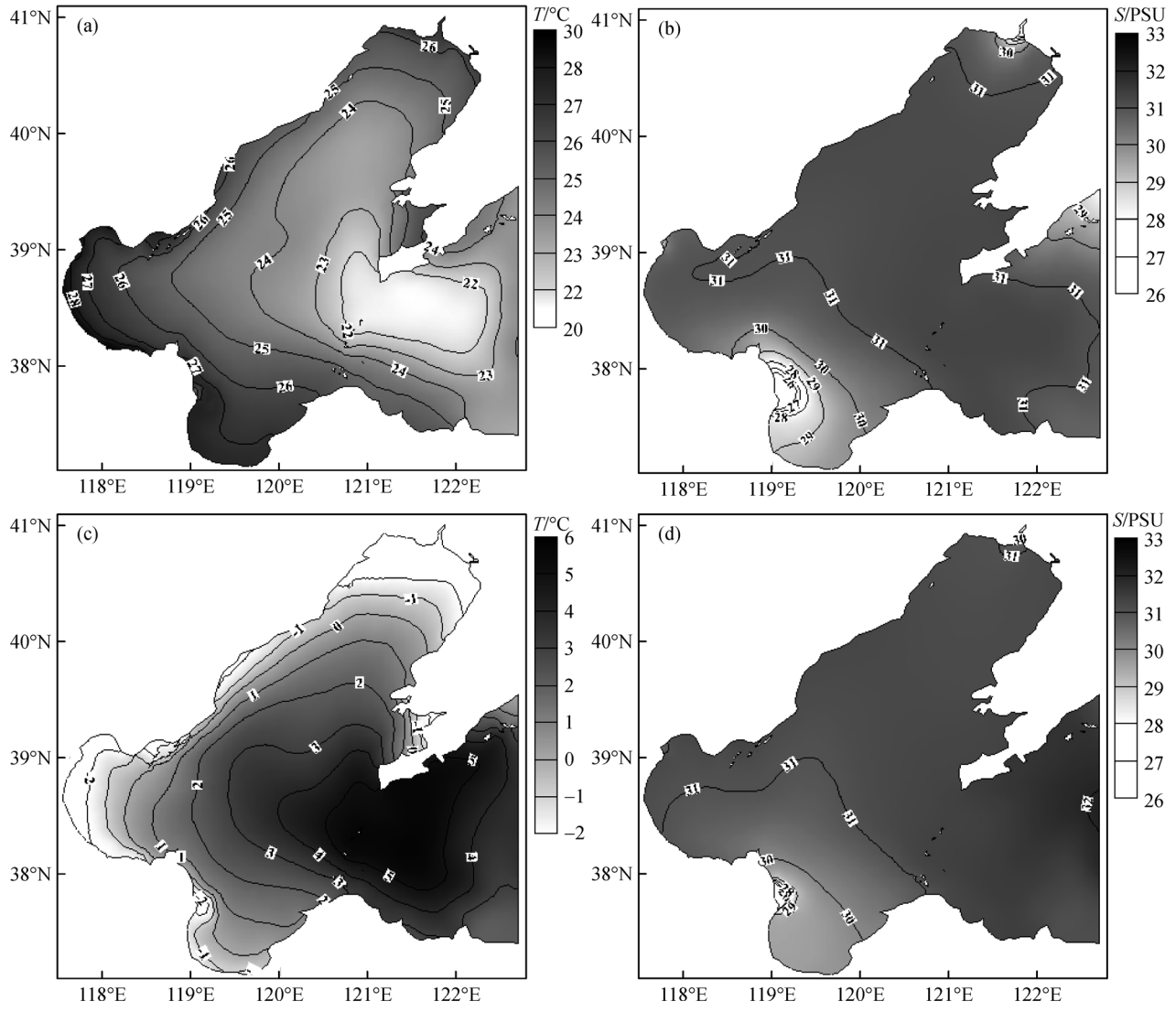

Fig. 8 The distribution of (a,c) temperature and (b,d) salinity during the summer (upper) and winter (lower) in the Bohai Sea.

Table 3 Regression analysis of temperature and salinity between simulation result and measured data

Measured station	Temperature		Salinity	
	RMSE/°C	R^2	RMSE/PSU	R^2
C1	2.0159	0.9333	0.1157	0.8488
C2	1.4843	0.9781	0.0662	0.8306
C3	1.1961	0.9848	0.2162	0.8779
C4	1.1514	0.9783	0.0375	0.9123

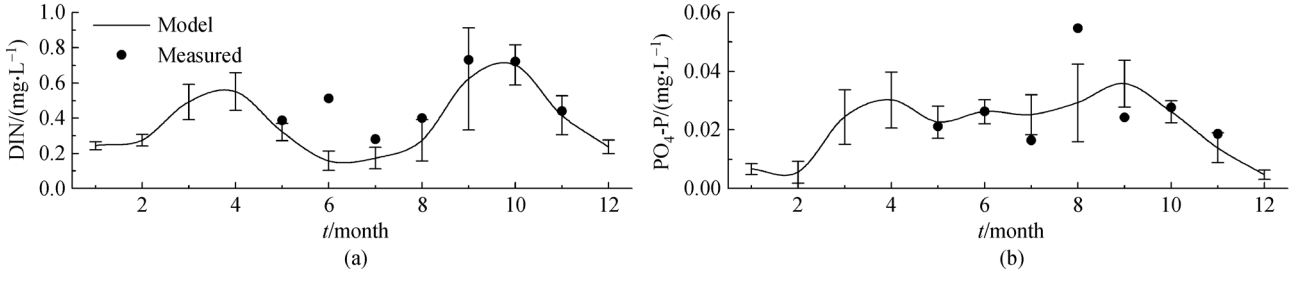

Fig. 9 The simulation results of (a) DIN and (b) PO_4-P in red tide monitoring area of Tianjin (Error bar represent standard deviation).

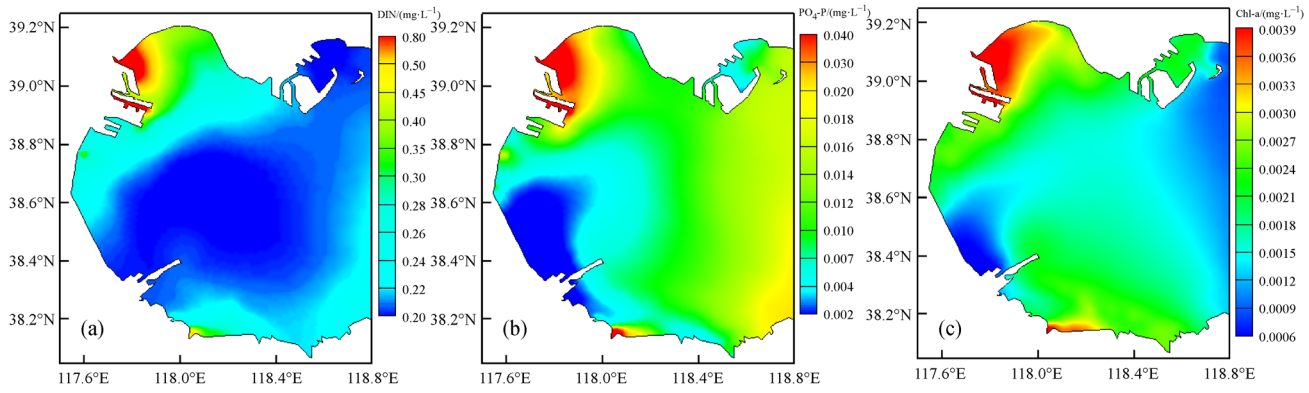

Fig. 10 The distribution of (a) DIN, (b) PO_4-P, and (c) Chl-a in the spring in Bohai Bay.

Table 4 Measured (Li et al., 2012) and simulated data of N/P at the measuring stations of Bohai Bay

Measured station	Longitude/°E	Latitude/°N	Measured/n(N) : n(P)	Model/n(N) : n(P)
E1	118.057	39.018	47.75	40.273
E2	118.215	38.958	51.58	47.706
E3	118.314	38.884	43.48	47.794
E4	118.591	38.778	43.48	32.121
E5	118.066	38.650	63.19	63.670
E6	118.318	38.502	58.74	49.652
E7	118.590	38.511	32.37	32.797
E8	118.068	38.381	114.5	100.97
E9	118.151	38.257	94.99	92.743
E10	118.324	38.258	67.12	48.060
E11	118.595	38.274	34.62	29.968

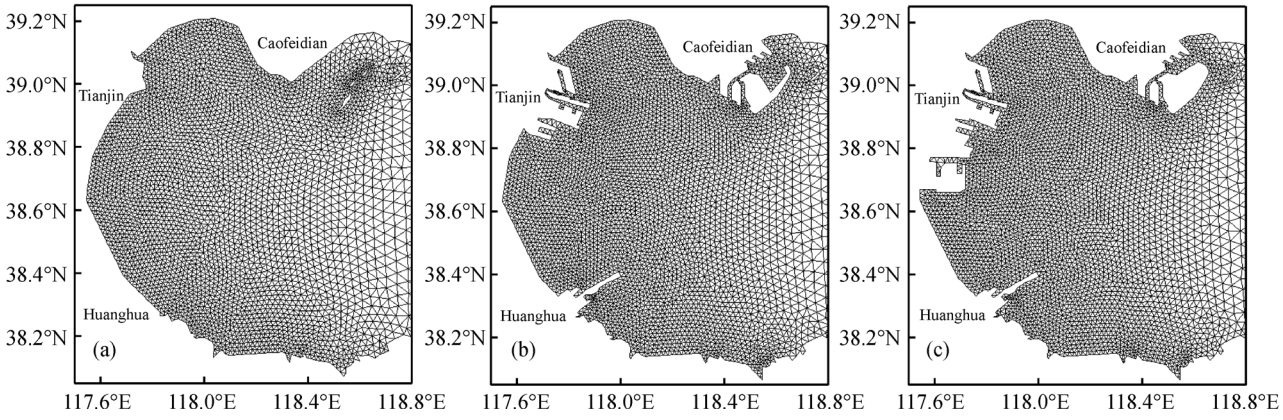

Fig. 11 Grids of different shorelines in Bohai Bay. (a) Grid 1: the natural shoreline in 2003; (b) Grid 2: the shoreline in 2011; (c) Grid 3: the expected shoreline in 2020.

the establishment of Tianjin Port, the reclamation has limited the Haihe River runoff to the surrounding area, leading to a change in the surrounding water flow field, salinity field, and various water quality parameters. Further detailed analysis is given in the following sections.

4.2 Influence of residual current

Tidal movement is the main dynamic process in Bohai Bay. The residual current has a significant influence on the ecology, material transport, and pollutant diffusion and

distribution. Based on the time-averaged velocity components of several tidal periods during the summer in Bohai Bay, the Euler residual current distributions in the area under different shoreline topographies are obtained, as shown in Fig. 12.

As the figure shows, the coastal residual current flows in opposite directions in the northern and southern parts of the Tianjin Port. The clockwise coastal residual current flows from the northern part of Tianjin Port to the Caofeidian Sea area, and the counter-clockwise coastal residual current flows from the southern part of Tianjin Port to the northern part of Huanghua Port.

The influence of shoreline variation on the residual current field is described as follows. The Caofeidian reclamation project makes the residual current disappear near the shore area of Caofeidian. Due to the influence of reclamation, the clockwise circulation at the northern part of Tianjin Port disappears and the coastal residual current has a minimal effect. The reclamation on the southern part of Tianjin Port and the construction of Huanghua Port results in a decrease in the counter-clockwise coastal residual current between the southern part of Tianjin Port and the northern part of Huanghua Port. The construction of Huanghua Port also results in a decrease in the residual current in the southward sea area and generates a counter-clockwise circulation in the southern part of the harbour. As shown in Fig. 12, the reclamation projects between 2011 and 2020 focus on the Caofeidian and Tianjin Dagang ports. With the reclamation project, the residual current in the north of Caofeidian Port and between Tianjin Dagang and Huanghua ports is further weakened.

4.3 Influence of tidal prism

Tidal prism refers to the volume of tidal water that can be accepted by the gulf. The size of the tidal prism reflects the self-purification capacity of the bay and determines the intensity of the water exchange between the bay and external bodies of water. The general formula for the tidal prism is:

$$W = \frac{1}{2}(S_1 + S_2)H, \tag{10}$$

where S_1 and S_2 are water areas at the times of high and low tide, respectively, and H is the tidal range. For the numerical simulation, the formula can be extended to:

$$W = \sum_{i=1}^{n} S_i(h_{1i} - h_{2i}), \tag{11}$$

where S_i is the area of elements, h_{1i} and h_{2i} are high and low tide level, and n is the number of elements. The calculation results and comparison are shown in Table 5. The statistical data on the tidal prism are consistent with the results of the remote sensing analysis by Ye et al. (2011). Compared with the situation in the three types of coastlines, the Bohai Bay area is gradually reduced because of the reclamation project, thereby leading to the gradual decrease of the tidal prism. The reduction of the tidal prism means that the water exchange volume between the internal and external water body of the bay decreases at the same time. Meanwhile, due to the shallow water in the area where the shoreline changes, the effect of reducing

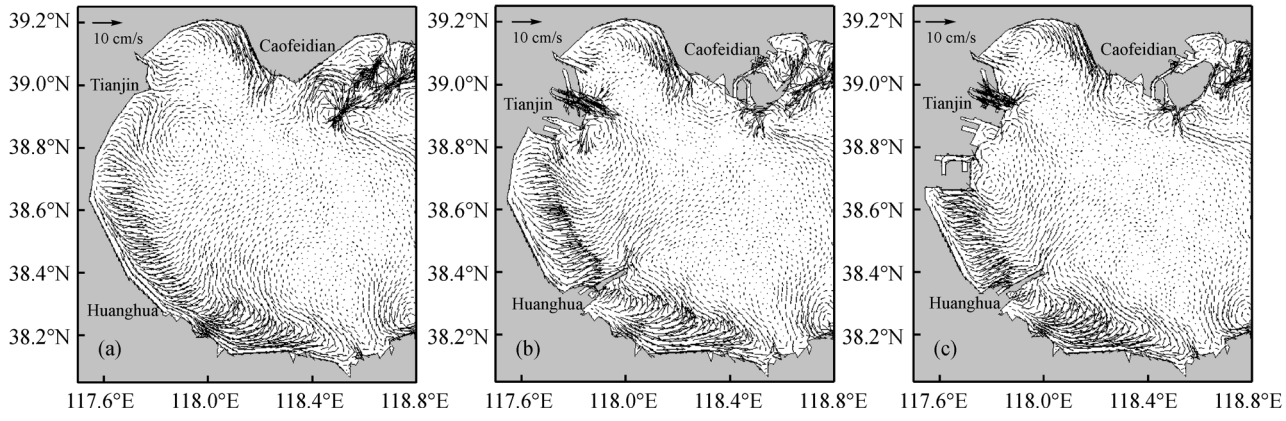

Fig. 12 The distribution of residual current in (a) Grid 1; (b) Grid 2; and (c) Grid 3 of Bohai Bay.

Table 5 Statistics and comparison of tidal prism in Bohai Bay

Source	Sea area/km^2	Tidal prism/(10^{10} m^3)	Change/(10^{10} m^3)	Rate of change/%
Reference (Ye et al., 2011)	—	2.99	—	—
Grid 1	10659	2.982	—	—
Grid 2	10163	2.825	−0.157	−5.26
Grid 3	9889	2.714	−0.268	−8.99

the total volume of water caused by reclamation is not obvious. The aforementioned two aspects lead to the weakening of the water exchange capacity of the bay, thereby reducing the ability of pollutants to spread out to the bay and weakening the self-purification capacity of sea water, which may lead to increased water pollution in the bay.

4.4 Influence of salinity

The distribution of salinity in different shorelines of Bohai Bay in summer is shown in Fig. 13. The distribution characteristics are as follows: salinity in estuaries is generally lower than 30 PSU and has a large gradient, but in the central and eastern areas, salinity is higher and the gradient is small. The influence of shoreline change on salinity distribution is mainly near the estuary. Comparison of the salinity distribution of Grids 1 and 2 shows that the construction of Tianjin Port affects the runoff of the Haihe River and weakens the dilution effect of the river on seawater, thereby resulting in the increase of salinity in the south of Tianjin Port. The construction of Huanghua Port blocks the spread of coastal residual current, resulting in an increase of salinity in this area. Comparison of the salinity distribution of Grids 2 and 3 shows that the reclamation further blocks the coastal residual current and weakens the runoff dilution effect, leading to a further increase in the salinity in the southwestern part of the bay.

4.5 Influence of water quality

To study the effect of reclamation on water quality, the simulation results of the entire domain were selected and averaged. The monthly averaged change curves of DIN, PO_4-P, and Chl-a in different shorelines of Bohai Bay are shown in Fig. 14. With the change of shoreline, the concentrations of PO_4-P and Chl-a increase and the concentration of DIN decreases.

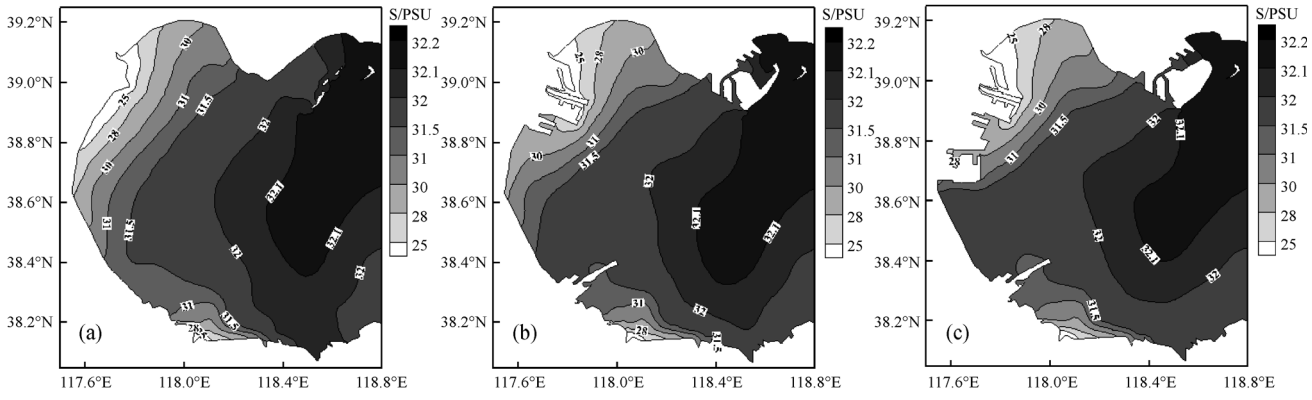

Fig. 13 The distribution of salinity in (a) Grid 1; (b) Grid 2; and (c) Grid 3 of Bohai Bay in summer.

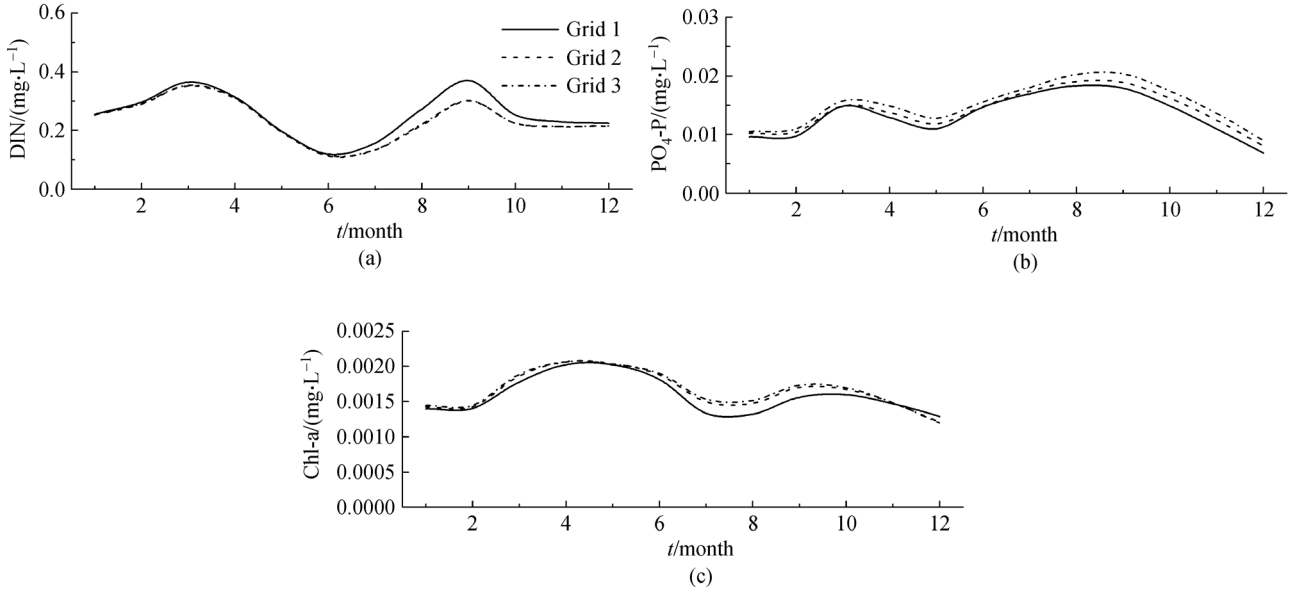

Fig. 14 Monthly averaged change curves of (a) DIN, (b) PO_4-P, and (c) Chl-a in different shorelines of Bohai Bay.

The reasons for this change are as follows: Table 5 shows that the shoreline change resulted in a significant reduction of the tidal prism in Bohai Bay, which weakens the water exchange capacity inside and outside the bay. Meanwhile, the decrease of the coastal residual current results in an increase in the concentration of PO_4-P. According to the analysis of the nutrition structure in Table 4, Bohai Bay has a phosphorus-limited nutrient structure, and the increase in PO_4-P leads to the growth of phytoplankton, that is, an increase in Chl-a concentration. Meanwhile, the growth of phytoplankton consumes a large amount of DIN, resulting in the decrease of DIN concentration. In addition, the construction of Tianjin Port blocks the diffusion of nutrients in the Haihe River, which is the largest runoff in the Bohai Bay area. The decrease in DIN during the flood season is more obvious than during other periods.

Table 6 shows the change of nutrient ratio at measuring stations. The N/P ratio of four points (E1, E5, E8, and E9) decreases by more than 10%, and all the four points are close to the shoreline change project area. By contrast, the points that are far from the engineering area (E4, E6, E7, and E11) have minimal change, which indicates that the change of the shoreline has a significant influence on the nutrient structure in the nearby sea area. The N/P ratio is generally decreased and the phosphorus restriction effect is weakened.

The distributions of DIN, PO_4-P, and Chl-a in different shorelines of Bohai Bay are shown in Fig. 15. The change of DIN distribution is described as follows: under the natural coastline, the high-value area appears near the estuary, and the distribution is mainly affected by runoff and decreased gradually to the centre and northeast of the bay. The construction of Tianjin Port weakens the runoff of the Haihe River and the concentration of the estuary area is slightly reduced due to blockage of the southern counter-clockwise coastal residual current, thereby resulting in lower concentrations in the southwestern part of the bay. In addition, the circulation in the south of Huanghua Port weakens the diffusion of DIN in this area, so that the concentration in this area has increased.

The change of PO_4-P distribution is similar to that of DIN. As Bohai Bay is a phosphorus-limited state, the PO_4-P concentration is scarce, so its distribution affected by runoff is more obvious. Furthermore, since the bay area and tidal prism are reduced, an increase in PO_4-P concentration is observed.

The change of Chl-a distribution is as follows: under the natural coastline, the high-value area appears near the estuary and in a centre to the north and south coast of a larger range, which is due to the coastal residual current in the area. The construction of Tianjin Port blocks the southern counter-clockwise coastal residual current, resulting in lower concentrations in the southwestern part of the bay. Meanwhile, the northern area of the bay is influenced by a clockwise residual current that results in higher concentrations. In addition, the construction of Huanghua Port blocks the coastal residual current and generates a counter-clockwise circulation in the southern area, resulting in higher concentrations in the southern part of Huanghua Port.

5 Conclusions

A hydrodynamic and water quality model in Bohai Bay is established to simulate the tide level, tidal current, temperature, salinity, and water quality in the area. The influence of shoreline changes on the coastal residual currents, tidal prism, salinity, and water quality caused by reclamation projects such as those at Tianjin, Caofeidian, and Huanghua ports is analysed.

As the reclamation project changes the shoreline of the estuary area, the runoff direction of the sea (u_s and v_s in

Table 6 Influence of shoreline changes on N/P

Measured station	Grid 1	Grid 2		Grid 3	
	n(N) : n(P)	n(N) : n(P)	Change	n(N) : n(P)	Change
E1	50.744	40.273	−10.47	37.229	−13.51
E2	56.063	47.706	−8.36	43.271	−12.79
E3	49.679	47.794	−1.89	43.927	−5.75
E4	31.550	32.121	0.57	31.770	0.22
E5	78.358	63.670	−14.69	59.055	−19.30
E6	48.495	49.652	1.16	48.451	−0.04
E7	32.760	32.797	0.04	32.407	−0.35
E8	111.94	100.97	−10.97	92.135	−19.80
E9	111.54	92.743	−18.79	81.901	−29.64
E10	52.465	48.060	−4.41	42.895	−9.57
E11	31.427	29.968	−1.46	27.013	−4.41

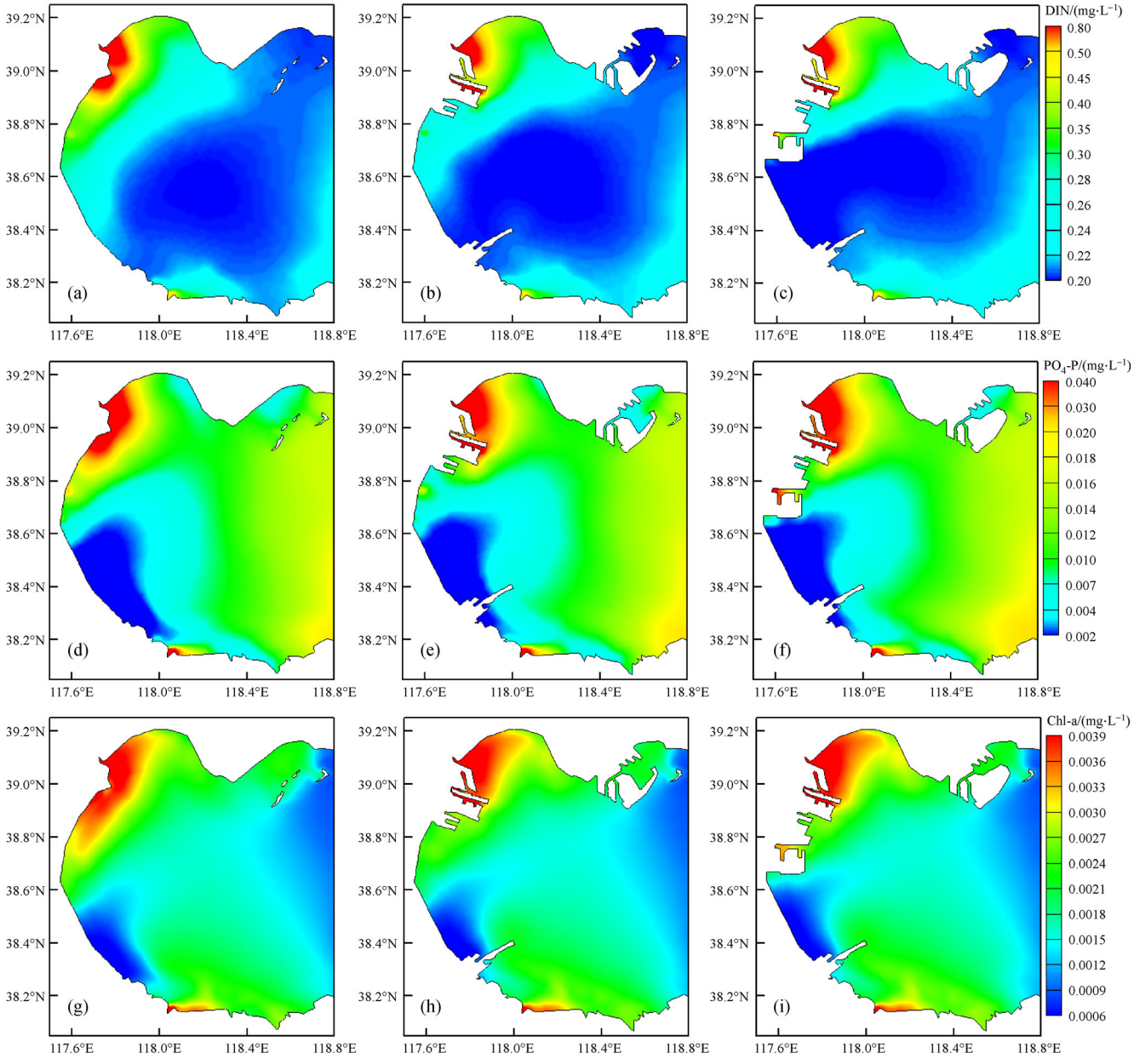

Fig. 15 The distribution of DIN (a, b, and c), PO_4-P (d, e, and f) and Chl-a (g, h, and i) in different shorelines of Bohai Bay.

Eqs. (2) and (3)) changes and the water flow direction is limited due to the limitation of the water grid, thereby leading to changes in flow velocity ($\overline{u}$ and $\overline{v}$ in Eqs. (2) and (3)). Based on these findings, $\overline{u}$ and $\overline{v}$ in transport equations (Eqs. (4)–(6)) change, thereby causing a change in temperature, salinity, and water quality parameters.

The following results are observed:

1) Shoreline changes weaken the residual current and generate a counter-clockwise circulation south of Huanghua Port, which results in weaker water exchange capacity and lower pollutant-diffusing capacity.

2) Shoreline changes reduce the area of Bohai Bay, resulting in a smaller tidal prism and further weakening the water exchange capacity. This condition is not conducive to the diffusion of pollutants, which may worsen the water pollution in the bay.

3) Shoreline changes hinder the spread of runoff, weaken the dilution effect of the river on seawater, and block the spread of coastal residual current, thereby resulting in increased salinity near the reclamation area.

4) Shoreline changes lead to an increase in PO_4-P concentration and decrease in DIN concentration. The value of N/P near the project decreases, which weakens the phosphorus-limited effect.

The impact of shoreline changes in Bohai Bay on the hydrodynamics and water quality of the surrounding area

is significant. The influence of the coastal residual current, tidal prism, and runoff leads to the weakening of the water exchange capacity and reduction of pollutant diffusion capacity. However, the influence is limited and the offshore area has a smaller impact.

Acknowledgements This study was funded by the National Natural Science Foundation of China (Grant No. 51779039).

References

Bao X W, Gao G P, Yan J (2001). Three dimensional simulation of tide and tidal current characteristics in the East China Sea. Oceanol Acta, 24(2): 135–149

Cai W Q, Borja Á, Liu L, Meng W, Muxika I, Rodríguez J G (2014). Assessing benthic health under multiple human pressures in Bohai Bay (China), using density and biomass in calculating AMBI and M-AMBI. Mar Ecol (Berl), 35(2): 180–192

Huai W X, Peter S Y, Komatsu T (2003). Hybrid finite analytic solutions of shallow water circulation. Appl Math Mech, 24(9): 1081–1088

Huai W X, Zeng X H, Komatsu T (2005). Numerical simulation of residual circulation due to bottom roughness variability under tidal flows in a semi-enclosed bay. China Ocean Eng, 19(4): 601–612

Kuang C P, Chen S Y, Zhang Y, Gu J, Deng L, Pan Y, Huang J (2012b). A two-dimensional morphological model based on next generation circulation solver II: application to Caofeidian, Bohai Bay, China. Coast Eng, 59(1): 14–27

Kuang C P, Chen S Y, Zhang Y, Gu J, Pan Y, Huang J (2012a). A two-dimensional morphological model based on a next generation circulation solver I: formulation and validation. Coast Eng, 59(1): 1–13

Li G J, Ma Y L, Li W, Wang J, Wei H (2012). Distribution of inorganic nutrients and potential eutrophication assessment in Bohai Bay in spring. Journal of Tianjin University of Science and Technology, 27 (5): 22–27

Li K Y, Liu X B, Zhao X G, Guo W (2010). Effects of reclamation projects on marine ecological environment in Tianjin Harbor Industrial Zone. Procedia Environ Sci, 2: 792–799

Liu X Y, Gao Z Q, Ning J C, Lu Q (2014a). Dynamic analysis on coastline and sea reclamation in the region around Bohai based on remote sensing images. In SPIE Optical Engineering Applications. International Society for Optics and Photonics, 9221: 92210U1-6

Liu Y, Kan W J, Zhang Q F (2014b). Study of nutrients changes and characteristics of eutrophication in Tianjin red tide monitoring area for the past four years. Ocean Development and Management, 4: 83–85

Redfield A C (1958). The biological control of chemical factors in the environment. Am Sci, 46(3): 205–221

Tian B, Wu W T, Yang Z Q, Zhou Y (2016). Drivers, trends, and potential impacts of long-term coastal reclamation in China from 1985 to 2010. Estuar Coast Shelf Sci, 170: 83–90

Wang C, Lu G H, Wang P F, Wu H, Qi P D, Liang Y (2011a). Assessment of environmental pollution of Taihu Lake by combining active biomonitoring and integrated biomarker response. Environ Sci Technol, 45(8): 3746–3752

Wang P F, Zhang S H, Wang C, Lu J (2012). Effects of Pb on the oxidative stress and antioxidant response in a Pb bioaccumulator plant Vallisneria natans. Ecotoxicol Environ Saf, 78: 28–34

Wang W, Liu H, Li Y, Su J (2014). Development and management of land reclamation in China. Ocean Coast Manage, 102: 415–425

Wang X L, Cui Z G, Guo Q, Han X R, Wang J T (2009). Distribution of nutrients and eutrophication assessment in the Bohai Sea of China. Chin J Oceanology Limnol, 27(1): 177–183

Wang X M, Li H Y, Meng W Q (2011b). Ecological impacts of marine reclamation in Binhai New Area of Tianjin. In Bioinformatics and Biomedical Engineering, 2011 5th International Conference on. IEEE, 1–4

Yan H K, Wang N, Yu T L, Fu Q, Liang C (2013). Comparing effects of land reclamation techniques on water pollution and fishery loss for a large-scale offshore airport island in Jinzhou Bay, Bohai Sea, China. Mar Pollut Bull, 71(1–2): 29–40

Yang H Y, Chen B, Barter M, Piersma T, Zhou C F, Li F S, Zhang Z W (2011). Impacts of tidal land reclamation in Bohai Bay, China: ongoing losses of critical Yellow Sea waterbird staging and wintering sites. Bird Conserv Int, 21(3): 241–259

Ye X M, Wang Q M, Ding J, Shi L J (2011). Satellite remote sensing investigation and analysis on the actuality of the tidal prism of bays in the Bohai Sea. Hydrographic Surveying and Charting, 31(6): 48–51

Zhao X, Sun Q (2013). Influence of reclamation on hydrodynamic environment in Bohai Bay. Adv Mat Res, 726: 3262–3265